A partial hominoid innominate from the Miocene of Pakistan: Description and preliminary analyses

Michèle E. Morgan[a,1], Kristi L. Lewton[b,c], Jay Kelley[d,e], Erik Otárola-Castillo[b], John C. Barry[b], Lawrence J. Flynn[a,b], and David Pilbeam[b,1]

[a]Peabody Museum of Archaeology and Ethnology and [b]Department of Human Evolutionary Biology, Harvard University, Cambridge, MA 02138; [c]Department of Anatomy and Neurobiology, Boston University School of Medicine, Boston, MA 02118; [d]Institute of Human Origins and School of Human Evolution and Social Change, Arizona State University, Tempe, AZ 85287; and [e]Department of Paleobiology, National Museum of Natural History, Smithsonian Institution, Washington, DC 20560

Contributed by David Pilbeam, October 29, 2014 (sent for review February 12, 2014; reviewed by David M. Alba, Daniel L. Gebo, and Carol V. Ward)

We describe a partial innominate, YGSP 41216, from a 12.3 Ma locality in the Siwalik Group of the Potwar Plateau in Pakistan, assigned to the Middle Miocene ape species *Sivapithecus indicus*. We investigate the implications of its morphology for reconstructing positional behavior of this ape. Postcranial anatomy of extant catarrhines falls into two distinct groups, particularly for torso shape. To an extent this reflects different although variable and overlapping positional repertoires: pronograde quadrupedalism for cercopithecoids and orthogrady for hominoids. The YGSP innominate (hipbone) is from a primate with a narrow torso, resembling most extant monkeys and differing from the broader torsos of extant apes. Other postcranial material of *S. indicus* and its younger and similar congener *Sivapithecus sivalensis* also supports reconstruction of a hominoid with a positional repertoire more similar to the pronograde quadrupedal patterns of most monkeys than to the orthograde patterns of apes. However, *Sivapithecus* postcranial morphology differs in many details from any extant species. We reconstruct a slow-moving, deliberate, arboreal animal, primarily traveling above supports but also frequently engaging in antipronograde behaviors. There are no obvious synapomorphic postcranial features shared exclusively with any extant crown hominid, including *Pongo*.

Sivapithecus | innominate | Miocene hominoid | torso shape | positional behavior

The Miocene hominoid *Sivapithecus* is restricted to the Indian subcontinent, with the majority of specimens having been recovered from the Potwar Plateau, Pakistan. At present, almost all *Sivapithecus* material is classified into three species: *Sivapithecus indicus* (12.7–11.4 Ma), *Sivapithecus sivalensis* (~11–8.5 Ma), and *Sivapithecus parvada* (10.1 Ma) (1); a fourth possible species, *Sivapithecus simonsi* (2), may be represented by a small number of specimens. Based on plausibly assigned postcranial specimens, both *S. indicus* and *S. sivalensis* have estimated weights of ~30–45 kg for males and ~20–25 kg for females; the two species differ somewhat in dental size and proportions but are similar enough both dentally and postcranially to be interpreted as a single lineage (1, 3). We do not believe that possible differences in palatal morphology between the two species (1, 4–6) presently warrant their separation into different genera. *S. parvada*, known from a single Potwar locality (7), is substantially larger, with males and females estimated respectively at ~60–75 and ~30–45 kg. Based on a small dentognathic sample, *S. simonsi*, if a separate species, would be the smallest species of the genus (1–3, 8).

Innominates are rare in the catarrhine fossil record. Here we describe the first attributed to *Sivapithecus*, YGSP 41216, a left partial innominate assigned to *S. indicus*. (On loan from Pakistan and curated at Harvard University, the fossil was recovered in 1990 and identified as primate in 2010.) It is from a locality in the mid-Chinji Formation, Y647, dated by paleomagnetic correlation to 12.3 Ma (9). Locality Y647 is a complex large-scale fill of a major channel (10). Two nearby fossil localities at the same stratigraphic level, Y494 and Y496, were formed by the same channel and share the same depositional environment as Y647. *S. indicus* is present at all three localities, represented by the innominate, a partial maxilla (6), and three isolated teeth.

YGSP 41216 is similar in both size and general shape to the innominates of males of the cercopithecoid monkeys *Nasalis* and *Papio*; the individual from which the fossil came therefore likely fell within the 20- to 25-kg range and we consider it a probable female *S. indicus*.

There are clear differences in positional repertoires between extant catarrhine monkeys and apes (summarized in ref. 11). The former are pronograde quadrupedal runners and leapers whereas the latter use a range of antipronograde behaviors in addition to quadrupedal knuckle-walking in African apes (see *Supporting Information* for definitions). These contrasting behaviors are reflected in fundamentally different postcranial morphological adaptations. Of particular interest here are differences in torso shape: cercopithecoids and most ceboids have relatively narrow torsos, in contrast to the broader torsos of apes, and these differences are in turn reflected in differences in innominate shape (11). In cercopithecoid and ceboid innominates the ilia are relatively narrow and more sagittally oriented, in contrast to the relatively broad and more coronally oriented ilia of extant hominoids (Fig. S1). YGSP 41216 is therefore critical to interpreting torso shape and the positional repertoire of *Sivapithecus* and is part of a postcranium that adds to the morphological diversity of known Miocene hominoids.

Sivapithecus also figures prominently in debates concerning the evolutionary history of extant apes, with most studies favoring a close phylogenetic relationship with the orangutan, *Pongo* (4, 5,

Significance

The living apes share a number of important morphological similarities of torso and limbs; torsos are broad and shallow, lumbar regions short, and forelimbs adapted to mobility. For more than a century it was assumed that most of these similarities are homologous, reflecting descent from a common ancestor with these features. As the ape fossil record slowly expands, the story becomes more complicated, particularly in the case of the south Asian Miocene ape *Sivapithecus*. *Sivapithecus* has facial features resembling specifically the living orangutan, but no postcranial features resembling orangutans. This newly described hipbone differs from that of all living apes. Either postcranial similarities of apes are not fully homologous or the facial similarities of *Sivapithecus* and orangutans cannot be homologous.

Author contributions: M.E.M., K.L.L., and D.P. designed research; M.E.M., K.L.L., J.K., J.C.B., L.J.F., and D.P. performed research; M.E.M., K.L.L., J.K., E.O.-C., J.C.B., L.J.F., and D.P. analyzed data; and M.E.M., K.L.L., J.K., E.O.-C., and D.P. wrote the paper.

Reviewers: D.M.A., Institut Català de Paleontologia Miquel Crusafont, Universitat Autònoma de Barcelona; D.L.G., Northern Illinois University; and C.V.W., University of Missouri.

The authors declare no conflict of interest.

[1]To whom correspondence may be addressed. Email: memorgan@fas.harvard.edu or pilbeam@fas.harvard.edu.

This article contains supporting information online at www.pnas.org/lookup/suppl/doi:10.1073/pnas.1420275111/-/DCSupplemental.

12–16). Some facial and palatal features resemble the pattern seen only in *Pongo* (5, 12, 14), whereas certain postcranial elements reveal that *Sivapithecus* was very different from any extant great ape (17). Thus, whether one interprets *Sivapithecus* as a member of the *Pongo* clade, or merely as a stem hominid, the suite of craniofacial and postcranial features characterizing this genus reveals substantial homoplasy, either cranial or postcranial, during great ape evolution. If *Sivapithecus* is within the *Pongo* clade, the new innominate will add to our understanding of the nature and breadth of postcranial homoplasy among the extant apes.

Description

YGSP 41216 lacks nearly all of the pubis, the ilium cranial to the auricular surface, and the most caudal portion of the ischium (Fig. 1). Although fractured in a few places, the several parts retain their correct anatomical positions and there is no sign of plastic deformation. The specimen has little abrasion but does exhibit some cracking. There are at least two perimortem puncture marks on the proximal ilium, one dorsal and one ventral, which we attribute to a crocodilian based on the distinctive shape of the punctures (18).

The iliac blade is narrow, and the region between the hip and sacroiliac joints is robust in comparison with extant great apes (Fig. S1). Although ilium width is greater at the level of the auricular surface than at its junction with the acetabulum, iliac flare would not have been comparable to that in extant hominoids, including hylobatids. The orientation of the ilium relative to the ischiopubic plane (i.e., iliopubic angle) indicates a primarily parasagittally oriented ilium and narrow torso, as in most primates (and other mammals), rather than the more coronal orientation and associated broad torso of extant great apes and hylobatids.

The iliac fossa is predominantly smooth and flat; toward the caudal end it becomes very slightly concave as it approaches the anterior inferior iliac spine (Fig. 1*A*). The gluteal iliac surface is markedly transversely concave at its most cranial aspect, decreasing in concavity caudally, and becoming almost flat near the acetabular rim. The anterior inferior iliac spine is flange-like and rugose, its center 20.9 mm from the cranial acetabular rim.

The iliac tuberosity is robust throughout its preserved length, from the clearly defined posterior inferior iliac spine to above the level of the most cranial margin of the sacroiliac joint (Fig. 1 *A* and *C*). The posterior superior iliac spine is not preserved. The auricular surface is preserved in its entirety and is well delimited (Fig. 1*A*); the cranial limb is longer and narrower than the caudal limb. Cranial and caudal limbs differ in their articular curvatures, with the cranial being relatively flat and the caudal being mediolaterally convex. The greater sciatic notch is long and shallow, as in many cercopithecoids; viewed parasagittally it is sigmoidal in shape (Fig. 1*B*).

The acetabular floor is broken and there is some minor bone loss to the caudal lunate surface just dorsal to the acetabular notch (Fig. 1*D*). The lunate surface is extensive cranially, dorsally, and caudally and is separated from the acetabular floor by a groove, shallow cranially and deepening to ∼2 mm caudally.

The ischium is long and robust compared with that in extant great apes. Some parts of the contact with the tuberosity seem to be present. The flat posteromedial surface flares laterally caudal to the prominent, ridge-like ischial spine (Fig. 1 *B* and *C*). A rounded ridge extending caudally from the spine separates the medial and lateral ischial borders. The lateral surface is convex. The angle and degree of flare in the preserved body of the ischium (Fig. 1 *B* and *C*) are not compatible with the presence of a flattened tuberosity and ischial callosity (Fig. S1).

Although the majority of the pubis is missing, the lateral-most portion of the superior pubic ramus is preserved, including the iliopubic eminence.

Comparative Morphology

Principal components analysis (PCA) of 16 variables (Table 1, variables 1–7 and 9–17) from extant anthropoids in dataset 1 of Table 2 and fossil specimens summarize phenetic similarities among fossil and extant species (*Methods*). The first two principal components are plotted for all individuals in Fig. 2; Euclidean distances based on group means are provided in Table S1 and centroids are in Table S2.

Sivapithecus is most similar to atelines in general (Fig. 2) and to *Lagothrix* in particular (Table S1). *Proconsul*, an African early Miocene probable stem hominoid, is closest to *Sivapithecus*, and then equally to *Lagothrix* and some cercopithecoid monkey species by Euclidean distance, but clusters with the cercopithecoid individuals lying closest to the atelines in the principal components

Fig. 1. Ventromedial (*A*), dorsal (*B*), dorsolateral (*C*), and lateral (*D*) views of YGSP 41216, a partial left innominate.

Table 1. Measurements for YGSP 41216

No.	Variables*	Value†
1	Ischial length (HL)	75‡
2	Lower iliac height (LIH)	68.7
3	Maximum iliac blade width (IW)	52.4
4	Iliac tuberosity width (ITW)	27.5
5	Iliac sacral surface width (ISW)	35.8
6	Dorsal acetabular wall minimum (DAW)	20.0
7	Ventral acetabular wall minimum (VAW)	16.1
8	Acetabular length (AL)	32.6
9	Acetabular depth (AD)	19.7
10	Acetabular notch width (ANW)	19.6
11	Cranial lunate surface width (CLS)	17.6
12	Dorsal lunate surface width (DLS)	10.1
13	Caudal lunate surface width (ULS)	12.6
14	Maximum ischial ramus width (XHRW)	22.0
15	Minimum ischial ramus width (NHRW)	14.2
16	Ischial tuberosity width (XHTW)	14‡
17	Iliopubic angle	101°
18	Ischial ramus length (ISCHL)	58.1
19	Lower ilium cross-sectional area (LICSA)	276.9 mm^2

*Measurements defined in *Supporting Information* from Ward (19) and Lewton (20, 21).
†Measurements are in millimeters unless otherwise noted.
‡Conservative estimate based on preserved portion.

plot. The African Plio-Pleistocene cercopithecoid monkeys *Theropithecus oswaldi* and *Paracolobus chemeroni* fall with the extant catarrhine monkey group.

Differences between the extant groups are driven by differences in iliopubic angle, iliac breadth, hip joint dimensions, and ischial robusticity. Variables loading heavily on principal component 1, which explains 67% of sample variation and separates *Sivapithecus* from the siamangs and great apes, are iliopubic angle and ilium width dimensions (IW, ITW, and ISW) (Table 3). Principal component 2 (explaining 16% of variation) separates *Sivapithecus*, *Hylobates*, *Symphalangus*, and atelines from the catarrhine monkeys and the majority of great ape individuals and is driven by ischium dimensions (HL and XHTW) and iliac breadth dimensions (IW and ITW). As is commonly the case, principal component 1 also reflects size, with larger species falling at the positive end of the axis.

Sivapithecus, like *Proconsul* (11, 22), exhibits a narrow, non-great ape-like ilium, with an iliac sacral surface width (ISW) that falls just outside the range of extant cercopithecoid monkeys but within that of the fossil monkeys (Fig. S2). Extant monkeys and great apes have nonoverlapping ISW dimensions. However, iliac tuberosity width (ITW) is narrower in *Sivapithecus* than in *Proconsul* or the fossil cercopithecoid monkeys (taxa with similar ISW) and is closest to the values of the majority of extant cercopithecoids.

The lower ilium of *Sivapithecus* is robust. Its cross-sectional area (LICSA) relative to acetabulum length (our proxy for body size) is similar to that of *Proconsul* (Fig. S3 and Table S3). Both fossil taxa have larger LICSAs than expected for their acetabulum lengths compared with extant anthropoids, with *Sivapithecus* having the largest positive residual among all taxa in the sample. Extant apes fall on or below the regression line and most have negative residual values (Fig. S3).

The acetabulum of *Sivapithecus* is deep and steep-sided (Fig. 1*D*). Relative to acetabular length, acetabular depth in *Sivapithecus* is greater than in *Proconsul* and greater than expected from the anthropoid regression (Figs. S1 and S4 and Table S3). It is similar to the majority of cercopithecoids in this respect. Cranial lunate surface size is also larger in *Sivapithecus* than in *Proconsul*, *Theropithecus*, and *Paracolobus* (all similar to each other in innominate and estimated body size). This aligns *Sivapithecus* with extant hominoids and platyrrhines (positive residuals), whereas *Proconsul* and the two fossil monkeys align with extant cercopithecoids (generally negative residuals) (Fig. S5*A* and Table S3). As has been shown (22), in extant great apes the cranial lunate surface is expanded relative to the dorsal surface compared with monkeys; *Sivapithecus* plots with extant great apes whereas *Proconsul* plots closest to large fossil monkeys (Fig. S5*B*)

The preserved anatomy of the distal ischium, particularly ischial tuberosity width (XHTW), indicates that *Sivapithecus* did not have a large ischial tuberosity. In relative XHTW, both *Sivapithecus* and *Proconsul* are similar to atelines and great apes and unlike hylobatids and cercopithecoids (Fig. S6 and Table S3).

Although the pubis is largely lacking in YGSP 41216, we are confident in estimating the iliopubic angle from the preserved ischium and proximal pubis. The iliopubic angles of both *Sivapithecus* (101°) and *Proconsul* (107°) (19) fall within the ranges of both New and Old World monkeys, distant from those of extant apes (Fig. S7). Extant apes have very low angles, between 62° and 73° in this sample, reflecting relatively broad torsos, whereas monkeys have iliopubic angles between 84° and 113°, reflecting relatively narrow torsos (11, 23).

Table 2. Numbers of individuals in extant primate comparative samples

	Dataset 1*			Dataset 2†		
Genus and species	♂	♀	Unknown	♂	♀	Unknown
Alouatta caraya				10	10	
Alouatta spp.	8	2				
Ateles spp.	8	8	1	11	9	1
Cebuella pygmaea				7	5	
Cebus albifrons				7	8	
Cebus apella	2	2		14	8	
Cercocebus torquatus				5	5	1
Cercopithecus mitis				10	13	1
Chlorocebus aethiops				10	9	1
Colobus guereza	9	10		7	12	4
Erythrocebus patas	1	3		3	1	2
Gorilla gorilla	10	10		11	10	
Homo sapiens				20	20	
Hylobates hoolock				7	6	
Hylobates lar	10	10		13	11	
Lagothrix lagotricha	6	2		6	3	1
Leontopithecus spp.				9	10	
Lophocebus albigena	4	3				
Macaca fascicularis	10	10		21	13	3
Macaca nemestrina				9	3	1
Mandrillus sphinx				4	3	1
Miopithecus talapoin				4	11	
Nasalis larvatus	6	10		11	7	2
Pan paniscus	8	10				
Pan troglodytes	10	10		20	21	
Papio cynocephalus	10	10				
Papio spp.				23	14	8
Pongo pygmaeus	6	10		15	2	2
Presbytis cristata	10	10				
Presbytis rubicunda	10	10				
Procolobus badius	3	10		5	5	
Saimiri spp.				10	10	
Symphalangus syndactylus	2	5	3	2	8	
Theropithecus gelada				1	5	

These datasets were not combined in any analyses and include overlapping individuals.
*Data collected by Ward (19) with additions to *Alouatta*, *Ateles*, *Cebus*, and *Symphalangus* by authors J.C.B., J.K., and M.E.M. (see Dataset S1).
†Data collected by Lewton (20, 21).

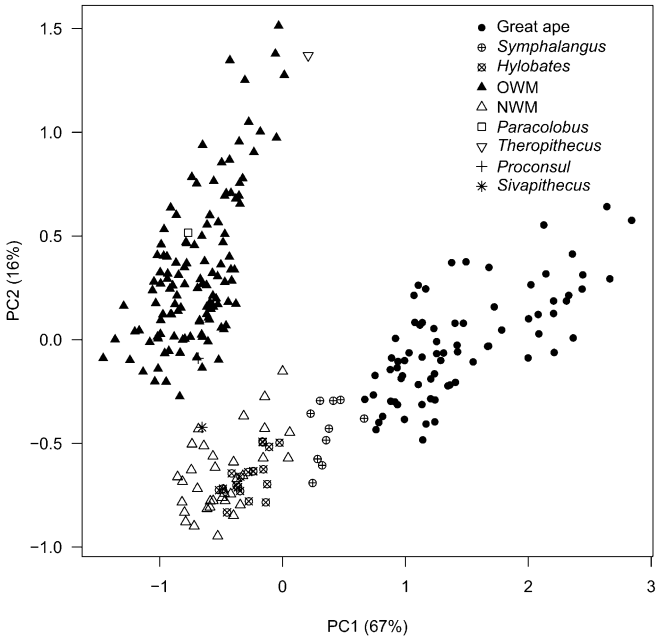

Fig. 2. Bivariate plot of principal components 1 and 2. Sample derives from dataset 1 but excludes *Colobus* and *Cebus* owing to missing data. Fossil data included are from Table 1 and Ward (19).

Discussion

***Sivapithecus* Postcrania: Function and Behavior.** In overall morphology, the *Sivapithecus* innominate indicates positional behaviors primarily involving pronograde quadrupedalism.

The large iliopubic angle of YGSP 41216 reflects a relatively narrow torso with iliac blades oriented parasagittally, similar to extant cercopithecoid and ceboid monkeys. The coronally positioned ilia of apes correlate with chest indices (ratio of chest breadth to depth) >120 (23). Extant ceboids have chest indices around 100, whereas those of cercopithecoids are <100 (23). Based on the correlation of chest index with iliopubic angle in the extant primate sample (Fig. S7), *Sivapithecus* likely had a chest index between 90 and 100.

The *Sivapithecus* innominate is generally robust, especially the ilium. The cross-sectional area of the lower ilium (i.e., iliac isthmus) is large relative to acetabulum size, as in *Proconsul* and larger ceboids. Lower ilium robusticity has long been thought to reflect bony adaptation to resisting loads incurred during positional behaviors (24–27), and recent work demonstrates a positive relationship between locomotor forces and lower ilium robusticity in strepsirrhines (28). Thus, for a primate of its size, *Sivapithecus* has a robust iliac isthmus that suggests the ilium was adapted to resist large loads, resulting from ground reaction or body weight forces. In addition, the convexity of the caudal limb of the auricular surface of the ilium and the robusticity of the iliac tuberosity suggest a possibly stable, iliosacral locking mechanism in *Sivapithecus* (albeit different from that in humans) (29); we have also observed this in *Proconsul*.

Ischial tuberosity width is related to the presence or absence of ischial callosities. Primates with ischial callosities (cercopithecoids and hylobatids) form one group in this measure, whereas those lacking callosities (platyrrhines and hominids) form another (30). *Sivapithecus* strongly aligns with the latter group.

Relative to its length, the acetabulum is deep in *Sivapithecus* and the entire lunate surface provides substantial articular surface area for the femoral head. In acetabular depth, *Sivapithecus* resembles cercopithecoid monkeys, whereas in lunate surface coverage it resembles atelines and great apes (Figs. S1, S4, and S5). This unusual combination of features, together with a femoral head morphology (preserved in *S. sivalensis*) that is spherical and evenly covered with articular surface (8), suggests a mobile, yet quite stable, hip joint that sustained loading from multiple directions.

Among other *Sivapithecus* postcranial elements, humeral shaft morphology closely resembles that of cercopithecoids (31), confirming the predominantly pronograde positional behavior implied by the narrow torso inferred from YGSP 41216. Other *S. indicus* and *S. sivalensis* postcranial specimens (3, 8, 17, 31–35) also sample a postcranium adapted to a kind of pronograde quadrupedalism. In most respects, the *Sivapithecus* postcranium is fundamentally like that of *Proconsul,* but with indications of greater mobility combined with stability at limb joints, including the hip, knee, and ankle joints (3, 8, 17).

Kelley (36) discussed the adaptive significance of, primarily, the *Proconsul* postcranium, noting evidence of powerful hand and foot grasping combined with forelimb and hindlimb joint mobility that was greater than in extant cercopithecoids. These were interpreted as adaptations necessary in a tailless arboreal ape of large body size to maintain balance while moving above branches. We assume that *Sivapithecus* also lacked an external tail and was therefore subject to the same challenges as *Proconsul* during arboreal locomotion. In the absence of a tail used as a counterweight (37), balance would have been maintained by maneuvering the torso, and therefore the center of gravity, from secure hand and foot holds, with hands and feet in a variety of orientations.

The combined evidence therefore suggests that *Sivapithecus* was a large, tailless, probably cautious and deliberate, arboreal pronograde quadruped, moving in a complex 3D environment. It likely adopted a wide variety of frequently abducted limb positions and might well on occasion have used various antipronograde positional behaviors, including suspension from three or more limbs as well as vertical climbing (3, 17). However, suspensory behaviors with fully extended and abducted forelimbs are less likely. In all of these behaviors, maintaining balance would have been critical and a particular challenge in a large quadruped lacking a tail. Many of the postcranial features in *Sivapithecus* can be coherently viewed in this context.

Innominate and Torso Morphology of Other Miocene Hominoids. The Early Miocene *Proconsul nyanzae* (~18 Ma) probable male innominate is almost complete, relatively long and narrow, and would have been oriented parasagittally (11). Associated vertebral remains record a long lumbar region with six traditionally

Table 3. Principal component loadings, with percentage contributions to sample variation

Variable	PC1 (67%)	PC2 (16%)	PC3 (8%)	PC4 (3%)
Iliopubic angle (radians)	−0.24	0.11	−0.01	−0.14
HL/AL	−0.07	0.25	0.11	−0.04
LIH/AL	−0.06	−0.09	0.31	0.03
IW/AL	0.53	0.20	0.02	−0.02
ITW/AL	−0.29	0.17	0.04	−0.01
ISW/AL	0.82	0.01	0.02	0.00
DAW/AL	0.02	0.09	0.01	0.00
VAW/AL	0.01	0.03	0.00	0.03
AD/AL	0.00	0.04	0.01	0.02
ANW/AL	−0.02	0.02	0.02	0.02
CLS/AL	0.06	0.00	0.01	0.00
DLS/AL	0.03	0.03	0.01	−0.01
ULS/AL	−0.01	0.02	0.01	0.00
XHRW/AL	−0.03	0.06	0.03	−0.01
NHRW/AL	0.00	0.03	0.02	0.03
XHTW/AL	−0.13	0.22	−0.05	0.14

Principal components 1–4 account for 95% of sample variation. The 11 remaining principal components each account for 2% or less of sample variation.

defined lumbar vertebrae and at least one thoracic with lumbar-type zygapophyseal articulations. Other material shows that *Proconsul* lacked an external tail (38), a feature likely to be a cladistically and behaviorally important hominoid synapomorphy (36, 39). Sampled is an animal with a relatively narrow and long torso, reflecting a generally pronograde positional repertoire.

Middle Miocene *Nacholapithecus kerioi* (Kenya; ~15–16 Ma) preserves a fragmentary ischium that provides minimal information about torso anatomy, although other postcranial features suggest a narrow torso and predominantly pronograde positional behavior (40–43). Like *Proconsul*, *Nacholapithecus* lacked a tail (38).

The latest Middle Miocene ape *Pierolapithecus catalaunicus* (Spain; 11.9 Ma) (16) is represented by a fragmentary ilium and ischium (44). The preserved ilium suggests somewhat greater ilial breadth than in *Proconsul* (or probably *Nacholapithecus*), although probably less than in the geologically younger *Oreopithecus* (discussed below) and extant apes. Some lumbar features indicate a shortened and stiffened lower back; the acute costal angle of several ribs points to a rather broad and short torso (45). Other postcranial features, for example of the hand, indicate a mixture of orthograde and pronograde positional behaviors (45, 46).

Late Miocene *Oreopithecus bambolii* (Italy; 8.3–6.7 Ma) (47) resembles extant large hominoids and siamangs in having an innominate with a broad ilium, ribs with acute costal angles (48–51), a vertebral column with five (traditionally defined) lumbar vertebrae, and mediolaterally narrow sacral alae (52), collectively indicating a short and broad trunk. Limb proportions and joint morphology (49, 53) suggest that orthograde positional behaviors were frequent, as in extant hominoids.

A currently undescribed hominoid partial innominate from late Miocene Rudabánya, Hungary (~10 Ma) has a flaring iliac blade (54), although not to the extent seen in extant large apes.

We note here also two nonhominoid taxa, the Plio-Pleistocene cercopithecoids *Paracolobus chemeroni* and *Theropithecus oswaldi*, that are similar in size to the larger Miocene apes discussed above but possess tails (38, 55). The innominates of both resemble *Proconsul nyanzae* and extant cercopithecoids in their iliac shape, being relatively narrow and long (11). Importantly, they demonstrate that increased body size alone would not explain broader torsos in hominoids.

Phylogenetic Interpretations. The new *Sivapithecus* innominate does not help resolve the "*Sivapithecus* dilemma," that is, whether or not *Sivapithecus* is interpreted as a member of the *Pongo* clade (56). Certain facial and palatal features resemble the pattern seen only in *Pongo*, but there are no postcranial features that do so. Indeed, there are no postcranial features linking *Sivapithecus* to any particular crown hominid, although there are features, for example features of the distal humerus (8), that resemble those of crown hominids generally. However, these, although derived for at least crown hominoids, are likely plesiomorphic for hominids and not necessarily associated with orthograde posture and positional behaviors (36). Over the past two decades other Miocene hominoids such as *Pierolapithecus, Hispanopithecus*, and *Rudapithecus* have been described that also exhibit to varying degrees postcranial similarities to crown hominoids, but, in these instances, such features are clearly associated with orthograde postures or even suspensory behaviors specifically (15, 16, 57). These taxa have been variously regarded as hominids (16), hominines (15), or pongines (57).

It has been proposed that the postcranial similarities of extant hominoids are, to varying extents, homoplasies (e.g., refs. 16, 44, 45, and 58–62), as opposed to a view that they are mostly homologies (e.g., refs. 39, 51, and 63–65). If crown hominoid postcranial similarities are largely or entirely homoplasies, then *Sivapithecus* can be plausibly interpreted as the sister taxon to *Pongo* by invoking convergent postcranial evolution in, at least, hylobatids and African and Asian large apes. However, if the postcranial features of crown hominoids related to orthograde positional behaviors are convergent, doubts arise about phylogenetic interpretations of *Pierolapithecus, Hispanopithecus*, and *Rudapithecus* that assume postcranial similarities between them and extant hominoids to be homologies. We acknowledge that these interpretations also rest in part on aspects of cranial morphology that are regarded as indicating membership in Hominidae, or even the African ape-human clade (Homininae) specifically (15, 16, 45, 66–68). Importantly though, even if the phylogenetic significance of these cranial features has been correctly interpreted, postcranial convergence related to orthogrady may still have occurred between the African and Asian hominid lineages. As originally noted by Pilbeam and colleagues (ref. 31, p. 239), almost a quarter century later problems still remain with "the objective definition of characters, assessment of homology versus convergence as alternative explanations for similarity... and determination of whether character states are primitive or derived. We are not confident that biologically plausible procedures [currently] exist for unambiguously settling these issues."

What might usefully contribute to greater understanding about the phylogenetic placement of *Sivapithecus* in particular, and of Miocene apes in general? Advances in at least three areas may be helpful: interdisciplinary research on "molecular clocks" to achieve consensus on timing of the crown hominoid radiation, additional hominoid fossils from West and Central Africa in the 15–5 Ma interval and Southeast Asia in the 10–5 Ma interval to better identify the antecedents of the extant great apes, and directed functional genomic research on key phenotypic features (e.g., the axial skeleton) with the aim of increasing the relative likelihood of either homology or homoplasy as explanations for observed morphological similarities.

Methods

Measures and Measurement Error. Nineteen pelvic measures were used (Table 1). Definitions in *Supporting Information* are from Ward (19) and Lewton (20). Measures of YGSP 41216 were taken on separate occasions by two observers (K.L.L. and M.E.M.). Each variable was measured five times. Average intraobserver error (coefficient of variation of the five measurement trials) was 1.7, and average interobserver error was 2.3. The final values for YGSP 41216 are averages of the composite 10 trials.

Samples. The extant comparative sample used here derives from Ward (19) (dataset 1) and Lewton (20, 21) (dataset 2), the former supplemented with additional specimens measured by coauthors J.C.B., J.K., and M.E.M. (Dataset S1). (Table 2 contains a complete list of measured species.) Only adult individuals with fused epiphyses were included. Not all measures were available on all included specimens. All data for fossil specimens (*P. chemeroni*, *T. oswaldi*, *Cercopithecoides williamsi*, and *P. nyanzae*) were obtained from published values (19), except for measures 1, 18, and 19 for *P. nyanzae*, which we took on a high-quality cast of the original specimen (see *Supporting Information* for details).

Statistical Analyses. All analyses were performed on dataset 1 except for those on lower ilium cross-sectional area, which used dataset 2. Restricted maximum likelihood was used to impute missing data points. Differences in overall pelvic shape were assessed using principal components analysis on covariances of measure 17 and size ratios (variable/acetabulum length) of measures 1–7 and 9–16 (JMP, Version 10; SAS Institute Inc.) Distance matrix results were calculated using pairwise Euclidean distances between the average of each species' principal components scores. Reduced major axis regressions were conducted using the smatr software package in R (69). The natural log of several variables was regressed on ln-acetabulum length, a proxy for body size.

ACKNOWLEDGMENTS. We thank J. Chupasko and M. Omura for frequent access to primate collections curated at the Museum of Comparative Zoology, Harvard University. C. Ward generously shared data from her comparative sample of extant primates. We supplemented these data and thank the curators and collection managers at the American Museum of Natural History (E. Westwig and D. Lunde), National Museum of Natural History (L. Gordon), Field Museum of Natural History (B. Patterson and W. Stanley), Cleveland Museum of Natural History (Y. Haile-Selassie and L. Jellema), Natural History Museum (P. Jenkins and L. Tomsett), and the Muséum National d'Histoire Naturelle (C. Lefèvre, J. Lesur-Gebremariam, J. Cuisin, and J. Villemain). Funding was provided by National Science Foundation Grants BCS 0752575 and EAR 0958178, The Leakey Foundation, and the American School for Prehistoric Research, Harvard University.

1. Kelley J (2005) *Interpreting the Past: Essays on Human, Primate, and Mammal Evolution in Honor of David Pilbeam*, eds Lieberman DE, Smith RH, Kelley J (Brill Academic Publishers, Boston, MA), pp 123–143.
2. Kay RF (1982) *Sivapithecus simonsi*, a new species of Miocene hominoid, with comments on the phylogenetic status of the Ramapithecinae. *Int J Primatol* 3(2):113–170.
3. DeSilva JM, Morgan ME, Barry JC, Pilbeam D (2010) A hominoid distal tibia from the Miocene of Pakistan. *J Hum Evol* 58(2):147–154.
4. Begun DR, Güleç E (1998) Restoration of the type and palate of Ankarapithecus meteai: Taxonomic and phylogenetic implications. *Am J Phys Anthropol* 105(3): 279–314.
5. Pilbeam D (1982) New hominoid skull material from the Miocene of Pakistan. *Nature* 295(5846):232–234.
6. Raza SM, et al. (1983) New hominoid primates from the middle Miocene Chinji formation, Potwar Plateau, Pakistan. *Nature* 306(5938):52–54.
7. Kelley J (1988) A new large species of *Sivapithecus* from the Siwaliks of Pakistan. *J Hum Evol* 17(3):305–324.
8. Pilbeam D, Rose MD, Badgley C, Lipschutz B (1980) Miocene hominoids from Pakistan. *Postilla* 181:1–94.
9. Ogg JG, Ogg G, Gradstein FM (2008) *The Concise Geologic Time Scale* (Cambridge Univ Press, Cambridge, UK), p 150.
10. Behrensmeyer AK, Badgley C, Barry JC, Morgan ME, Raza SM (2005) *Interpreting the Past: Essays on Human, Primate, and Mammal Evolution in Honor of David Pilbeam*, eds Lieberman DE, Smith RJ, Kelley J (Brill Academic Publishers, Boston, MA), pp 47–62.
11. Ward CV (1993) Torso morphology and locomotion in Proconsul nyanzae. *Am J Phys Anthropol* 92(3):291–328.
12. Ward SC, Brown B (1986) Facial anatomy of Miocene hominoids. *Comparative Primate Biology, Vol. 1: Systematics, Evolution, and Anatomy*, eds Swindler D, Erwin J (Liss, New York), pp 413–452.
13. Moyà-Solà S, Köhler M (1995) New partial cranium of *Dryopithecus* Lartet, 1863 (Hominoidea, Primates) from the upper Miocene of Can Llobateres, Barcelona, Spain. *J Hum Evol* 29(2):101–139.
14. Begun DR, Ward CV, Rose MD (1997) *Function, Phylogeny and Fossils*, eds Begun DR, Ward CV, Rose MD (Plenum, New York), pp 389–415.
15. Kordos L, Begun DR (2002) Rudabánya: A late Miocene subtropical swamp deposit with evidence of the origin of the african apes and humans. *Evol Anthropol* 11(2): 45–57.
16. Alba DM (2012) Fossil apes from the Vallès-Penedès basin. *Evol Anthropol* 21(6): 254–269.
17. Madar SI, Rose MD, Kelley J, MacLatchy L, Pilbeam D (2002) New *Sivapithecus* postcranial specimens from the Siwaliks of Pakistan. *J Hum Evol* 42(6):705–752.
18. Njau JK, Blumenschine RJ (2006) A diagnosis of crocodile feeding traces on larger mammal bone, with fossil examples from the Plio-Pleistocene Olduvai Basin, Tanzania. *J Hum Evol* 50(2):142–162.
19. Ward CV (1991) Functional anatomy of the lower back and pelvis of the Miocene hominoid *Proconsul nyanzae* from Mfangano Island, Kenya. PhD thesis (The Johns Hopkins Univ, Baltimore).
20. Lewton KL (2010) Locomotor function and the evolution of the primate pelvis. PhD thesis (Arizona State Univ, Tempe, AZ).
21. Lewton KL (2012) Evolvability of the primate pelvic girdle. *Evol Biol* 39(1):126–139.
22. Ward CV, Walker A, Teaford MF, Odhiambo I (1993) Partial skeleton of Proconsul nyanzae from Mfangano Island, Kenya. *Am J Phys Anthropol* 90(1):77–111.
23. Schultz A (1956) *Primatologia*, eds Hofer H, Schultz AH, Starck D (Karger, Basel), pp 887–964.
24. Le Gros Clark WE (1955) *The Fossil Evidence for Human Evolution* (Univ of Chicago Press, Chicago).
25. Robinson JT (1972) *Early Hominid Posture and Locomotion* (Univ of Chicago Press, Chicago).
26. Steudel K (1981) Functional aspects of primate pelvic structure: A multivariate approach. *Am J Phys Anthropol* 55(3):399–410.
27. Lovejoy CO, Suwa G, Spurlock L, Asfaw B, White TD (2009) The pelvis and femur of *Ardipithecus ramidus*: The emergence of upright walking. *Science* 326(5949):e1–e6.
28. Lewton KL (2015) Pelvic form and locomotor adaptation in strepsirrhine primates. *Anat Rec* 298(1):230–248.
29. Gerlach UJ, Lierse W (1992) Functional construction of the sacroiliac ligamentous apparatus. *Acta Anat (Basel)* 144(2):97–102.
30. Rose MD (1974) Ischial tuberosities and ischial callosities. *Am J Phys Anthropol* 40(3): 375–383.
31. Pilbeam D, Rose MD, Barry JC, Shah SMI (1990) New *Sivapithecus* humeri from Pakistan and the relationship of *Sivapithecus* and *Pongo*. *Nature* 348(6298):237–239.
32. Rose MD (1984) Hominoid postcranial specimens from the middle Miocene Chinji Formation, Pakistan. *J Hum Evol* 13(6):503–516.
33. Rose MD (1986) Further hominoid postcranial specimens from the late Miocene Nagri Formation of Pakistan. *J Hum Evol* 15(5):333–367.
34. Rose MD (1989) New postcranial specimens of catarrhines from the Middle Miocene Chinji Formation, Pakistan: Descriptions and a discussion of proximal humeral functional morphology in anthropoids. *J Hum Evol* 18(2):131–162.
35. Rose MD (1993) *Postcranial Adaptation in Nonhuman Primates*, ed Gebo DL (Northern Illinois Univ Press, DeKalb, IL), pp 252–272.
36. Kelley J (1997) Paleobiological and phylogenetic significance of life history in Miocene hominoids. *Function, Phylogeny, and Fossils: Miocene Hominoid Evolution and Adaptations*, eds Begun DR, Ward CV, Rose MD (Plenum, New York), pp 173–208.
37. Larson SG, Stern JT, Jr (2006) Maintenance of above-branch balance during primate arboreal quadrupedalism: Coordinated use of forearm rotators and tail motion. *Am J Phys Anthropol* 129(1):71–81.
38. Nakatsukasa M, et al. (2004) Tail loss in *Proconsul heseloni*. *J Hum Evol* 46(6):777–784.
39. Keith A (1923) Hunterian Lectures ON MAN'S POSTURE: ITS EVOLUTION AND DISORDERS: Given at the Royal College of Surgeons of England. *BMJ* 1:451–454.
40. Ishida H, Kunimatsu Y, Takano T, Nakano Y, Nakatsukasa M (2004) *Nacholapithecus* skeleton from the middle Miocene of Kenya. *J Hum Evol* 46(1):69–103.
41. Senut B, et al. (2004) Preliminary analysis of *Nacholapithecus* scapula and clavicle from Nachola, Kenya. *Primates* 45(2):97–104.
42. Nakatsukasa M, Kunimatsu Y, Nakano Y, Ishida H (2007) Vertebral morphology of *Nacholapithecus kerioi* based on KNM-BG 35250. *J Hum Evol* 52(4):347–369.
43. Nakatsukasa M, et al. (2012) Hind limb of the *Nacholapithecus kerioi* holotype and implications for its positional behavior. *Anthropol Sci* 120(3):235–250.
44. Hammond AS, Alba DM, Almécija S, Moyà-Solà S (2013) Middle Miocene Pierolapithecus provides a first glimpse into early hominid pelvic morphology. *J Hum Evol* 64(6):658–666.
45. Moyà-Solà S, Köhler M, Alba DM, Casanovas-Vilar I, Galindo J (2004) Pierolapithecus catalaunicus, a new Middle Miocene great ape from Spain. *Science* 306(5700):1339–1344.
46. Almécija S, Alba DM, Moyà-Solà S (2009) *Pierolapithecus* and the functional morphology of Miocene ape hand phalanges: Paleobiological and evolutionary implications. *J Hum Evol* 57(3):284–297.
47. Rook L, Oms O, Benvenuti MG, Papini M (2011) Magnetostratigraphy of the late Miocene Baccinello-Cinigiano basin (Tuscany, Italy) and the age of *Oreopithecus bambolii* faunal assemblages. *Palaeogeogr Palaeoclimatol Palaeoecol* 305:286–294.
48. Schultz A (1961) *Vertebral Column and Thorax* (Karger, Basel).
49. Harrison T (1986) A reassessment of the phylogenetic relationships of *Oreopithecus bambolii* Gervais. *J Hum Evol* 15(7):541–583.
50. Rook L, Bondioli L, Köhler M, Moyà-Solà S, Macchiarelli R (1999) *Oreopithecus* was a bipedal ape after all: Evidence from the iliac cancellous architecture. *Proc Natl Acad Sci USA* 96(15):8795–8799.
51. Sarmiento EE (1987) The phylogenetic position of *Oreopithecus* and its significance in the origin of the Hominoidea. American Museum Novitates 2881 (Am Museum of Natural History, New York).
52. Russo GA, Shapiro LJ (2013) Reevaluation of the lumbosacral region of *Oreopithecus bambolii*. *J Hum Evol* 65(3):253–265.
53. Jungers WL (1987) Body size and morphometric affinities of the appendicular skeleton in *Oreopithecus bambolii*. *J Hum Evol* 16(5):445–456.
54. Ward CV, Begun DR, Kordos L (2008) New partial pelvis of *Dryopithecus brancoi* from Rudabánya, Hungary. *Am J Phys Anthropol* 135(Supp 46):218.
55. Birchette MG (1982) The postcranial skeleton of *Paracolobus chemeroni*. PhD thesis (Harvard Univ, Cambridge, MA).
56. Pilbeam DR, Young NM (2001) *Sivapithecus* and hominoid evolution: Some brief comments. *Evolution and Climatic Change in Europe Volume 2: Phylogeny of the Neogene Hominoid primates of Eurasia*, eds de Bonis L, Koufos GD, Andrews P (Cambridge Univ Press, Cambridge, UK), pp 349–364.
57. Moyà-Solà S, Köhler M (1996) A *Dryopithecus* skeleton and the origins of great-ape locomotion. *Nature* 379(6561):156–159.
58. Larson SG (1998) Parallel evolution in the hominoid trunk and forelimb. *Evol Anthropol* 6(3):87–99.
59. Lovejoy CO, Suwa G, Simpson SW, Matternes JH, White TD (2009) The great divides: *Ardipithecus ramidus* reveals the postcrania of our last common ancestors with African apes. *Science* 326(5949):100–106.
60. Straus WL, Jr (1949) The riddle of man's ancestry. *Q Rev Biol* 24(3):200–223.
61. Weidenreich F (1946) *Apes, Giants, and Man* (Univ of Chicago Press, Chicago).
62. Wood Jones F (1926) *Arboreal Man* (Edward Arnold & Co., London).
63. Huxley TH (1863) *Evidence As to Man's Place in Nature* (Williams & Norgate, London).
64. Pilbeam D (2002) *The Primate Fossil Record*, ed Hartwig WC (Cambridge Univ Press, Cambridge, UK), pp 303–310.
65. Young NM (2003) A reassessment of living hominoid postcranial variability: Implications for ape evolution. *J Hum Evol* 45(6):441–464.
66. Begun DR (2001) African and Eurasian Miocene hominoids and the origins of the Hominidae. *Hominoid Evolution and Environmental Change in the Neogene of Europe, Volume 2: Phylogeny of the Neogene Hominoid Primates of Eurasia*, eds de Bonis L, Koufos G, Andrews P (Cambridge Univ Press, Cambridge, UK), pp 231–253.
67. Kordos L, Begun DR (2001) A new cranium of *Dryopithecus* from Rudabánya, Hungary. *J Hum Evol* 41(6):689–700.
68. Moyà-Solà S, et al. (2009) A unique Middle Miocene European hominoid and the origins of the great ape and human clade. *Proc Natl Acad Sci USA* 106(24):9601–9606.
69. R Core Team (2013) R: A language and environment for statistical computing. (R Foundation for Statistical Computing, Vienna). Available at www.R-project.org/.

Supporting Information

Morgan et al. 10.1073/pnas.1420275111

SI Materials

Additional Description of YGSP 41216. The preserved iliac length measured from the acetabular center is 111 mm, and our best estimate of maximum iliac length is 130–135 mm. We believe this estimate to be reasonable, but note that the fraction of iliac height above the auricular surface varies considerably within and between species. The ilium is narrowest superior to the cranial margin of the acetabulum (31.0 mm wide). At the level of the posterior inferior iliac spine the ilium is 44.6 mm wide and at the midpoint of the auricular surface 52.4 mm wide.

Ilium length from the center of the acetabulum to the most caudal part of the auricular surface is 68.7 mm. Maximum iliac width and maximum iliac fossa width are estimated as 52.4 mm and 35.8 mm, respectively; maximum iliac tuberosity width is 27.5 mm. The iliac fossa and tuberosity planes are separated by the gently rounded arcuate line that becomes more prominent caudally, thickening to 15.8 mm at the level of the cranial rim of the acetabulum. The robust iliac tuberosity measures 15.5 mm thick mediolaterally at its maximum. The sacro-iliac joint is clearly delimited; at the most posterior aspect the auricular surface measures 21.5 mm craniocaudally, whereas the maximum width of the anterocranial portion is 10.2 mm and is separated from the iliac fossa by a crest, now damaged except at its most cranial part where it is prominent and rounded. Markings for the origin of erector spinae are present.

The origin of gluteus medius is visible just caudal to the broken cranial margin of the iliac fossa and extending onto the lateral surface of the iliac tuberosity. Markings are also present for the origins of the posteromedial gluteus minimus. The ventral iliac border is 74.1 mm from the cranial acetabular rim to the broken cranial end, with a 7.2-mm section missing (Fig. 1). On the robust anterior inferior iliac spine, muscle markings for rectus femoris are present. The iliofemoral ligament attachment is also visible.

The greater sciatic notch is 76.5 mm long from the posterior superior iliac spine to the ischial spine and 13.0 mm deep. In lateral view it is sigmoid-shaped, with the cranial third medially concave, the medial third straight, and the caudal third laterally concave. The border is 9.5 mm thick cranially but narrows caudally to 3.5 mm between the acetabulum and ischial spine.

The acetabular rim is 20.0 mm from the dorsal (ischial) border and 16.1 mm from the arcuate line. Adjacent to the acetabular notch, the bone forming part of the obturator foramen margin is mediolaterally 11.1 mm wide at the cranial edge. The acetabulum is not laterally displaced relative to the auricular surface of the ilium.

Positional Behavior Definitions from Madar et al. (1). ***Pronogrady.*** Pronogrady includes any quadrupedal locomotion taking place on a support or supports angled at <45° from horizontal (including the ground), in which the hands and feet grip on most supports, but may be used in plantigrade/palmigrade or digitigrade fashion on the largest supports. The animal's trunk lies roughly parallel to the support(s) on which the activity is taking place.

Pronograde quadrupedalism (also called quadrupedal walking and running) takes place along or across a single support.

Antipronogrady. Antipronogrady refers to all activities (such as climbing and suspension) in which either the upper or lower limbs, or both, are used in tension (2).

Vertical climbing. Orthograde, quadrupedal ascent and descent modes that take place on supports angled at >45° from horizontal. The animal's trunk is held approximately vertically, with hand and foot grips taken on one or more supports.

Quadrumanous suspension. This occurs when both hands and feet grasp a support, usually while the animal's trunk is held horizontally (*Ateles* and *Pongo*).

Methods, Analyses, and Results. As described in the text, the extant comparative sample derives from two separate datasets: dataset 1 [Ward (3) and Dataset S1] and dataset 2 [Lewton (4, 5)], the former augmented by additional measurements done by the authors. Data on all comparative fossil material are from Ward (3). All analyses except for the lower ilium cross-sectional area regression were performed using dataset 1. Measures 1–17 (Table 1) were available for *Paracolobus chemeroni* and *Theropithecus oswaldi*. Only two measures—iliac tuberosity width (ITW) and iliac sacral surface width (ISW)—were available for *Cercopithecoides williamsi*.

The root mean square error (RMSE) was calculated to estimate the SD of the residuals presented in Table S3 and to identify residual values falling outside one standard range of error (6):

$$\mathrm{RMSE} = \sqrt{\frac{\sum_{i=1}^{n} (\hat{y}_i - y_i)^2}{n}}.$$

Here n is the sample size, y_i is the i^{th} observed response value, and $\hat{y}_i$ represents the i^{th} value computed using the coefficients estimated using reduced major axis regression: b_0 and b_1.

Innominate Measure Definitions. All of the following measures are defined and illustrated in Ward (3) with the exception of iliopubic angle, ischial ramus length (ISCHL), and lower ilium cross-sectional area (LICSA) defined in Lewton (4).

Ischial length (HL) – measured from the center of the acetabulum to the most caudal extent of the ischium, in line with its long axis

Lower iliac height (LIH) – measured from the center of the acetabulum to the most caudal extent of the auricular surface

Maximum iliac blade width (IW) – maximum width of the iliac blade measured perpendicular to the dorsal ridge of the ilium

Iliac tuberosity width (ITW) – measured at same level as IW: width of the sacral plane of the ilium

Iliac sacral surface width (ISW) – measured at same level as IW: width of the iliac fossa

Dorsal acetabular wall minimum (DAW) – minimum thickness of the dorsal wall of the acetabulum, measured from the medial surface of the ischium to the inner surface of the acetabular rim

Ventral acetabular wall minimum (VAW) – minimum thickness of the ventral acetabular wall, measured from the iliopectineal line to the inner surface of the acetabular rim

Acetabular length (AL) – maximum diameter of the acetabulum, measured from the outer-most points of the acetabular rim in the ilio-ischial plane.

Acetabular depth (AD) – distance from the AL plane to the deepest point on the acetabular floor

Acetabular notch width (ANW) – width of the nonarticular acetabular notch measured parallel to AL, and taken just adjacent to the cranial and caudal lunate surfaces

Cranial lunate surface width (CLS) – width of the cranial lunate surface at level of the iliac border of acetabulum

Dorsal lunate surface width (DLS) – width of the dorsal lunate surface at level of the DAW measure

Caudal lunate surface width (ULS) – width of the caudal lunate surface at level of the ischial border of acetabulum

Maximum ischial ramus width (XHRW) – maximum width of the ischial ramus (usually roughly dorsoventral)

Minimum ischial ramus width (NHRW) – minimum width of the ischial ramus (usually roughly mediolateral)

Ischial tuberosity width (XHTW) – maximum ischial tuberosity width taken perpendicular to the long axis of the ischium

Iliopubic angle – angle between the plane defined by the anterior superior iliac spine and dorsal border of the ilium and the plane defined by the pubic symphysis and the deepest part of the concavity along the ischial buttress

Ischial ramus length (ISCHL) - measured from the caudal-most aspect of the acetabular rim to the caudal-most aspect of the ischium, in line with the long axis of the ischium

Lower ilium cross-sectional area (LICSA) – area of the triangle formed by the following points: (*i*) lateral-most point on the lateral aspect of the lower ilium at iliac isthmus; (*ii*) dorsal-most point on the dorsal aspect of the lower ilium, taken directly across from *i*; and (*iii*) medial-most point on the medial aspect of the lower ilium, taken directly across from points *i* and *ii*

1. Madar SI, Rose MD, Kelley J, MacLatchy L, Pilbeam D (2002) New *Sivapithecus* postcranial specimens from the Siwaliks of Pakistan. *J Hum Evol* 42(6):705–752.
2. Stern JT, Jr (1975) Before bipedality. *Yearb Phys Anthropol* 9:59–68.
3. Ward CV (1991) Functional anatomy of the lower back and pelvis of the Miocene hominoid *Proconsul nyanzae* from Mfangano Island, Kenya. PhD thesis (The Johns Hopkins Univ, Baltimore).
4. Lewton KL (2010) Locomotor function and the evolution of the primate pelvis. PhD thesis (Arizona State Univ, Tempe, AZ).
5. Lewton KL (2012) Evolvability of the primate pelvic girdle. *Evol Biol* 39:126–139.
6. Freedman D, Pisani R, Purves R (2007) *Statistics* (Norton, New York), 4th Ed.

Fig. S1. Dorsolateral (top) and ventromedial (bottom) views of left innominates of (*A*) *Pongo pygmaeus* (PMAE 96-6-60/59940.0), (*B*) *Pan troglodytes* (PMAE 58-60-50/N8518.0; mirror image of right innominate), (*C*) *Nasalis larvatus* (MCZ 37327), (*D*) *Proconsul nyanzae* (KNM-MW 13142D; cast), and (*E*) *Sivapithecus indicus* (YGSP 41216). Reference points are 1, anterior superior iliac spine; 2, posterior superior iliac spine; 3, posterior inferior iliac spine; 4, anterior inferior iliac spine; 5, lunate surface of acetabulum; 6, auricular surface; 7, greater sciatic notch; 8, iliac tuberosity; 9, iliac fossa; and 10, arcuate line. (PMAE 96-6-60/59940.0 and PMAE 58-60-50/N8518.0, Peabody Museum of Archaeology and Ethnology, Harvard University © 2014 President and Fellows of Harvard College; MCZ 37327, Museum of Comparative Zoology, Harvard University © 2014 President and Fellows of Harvard College.)

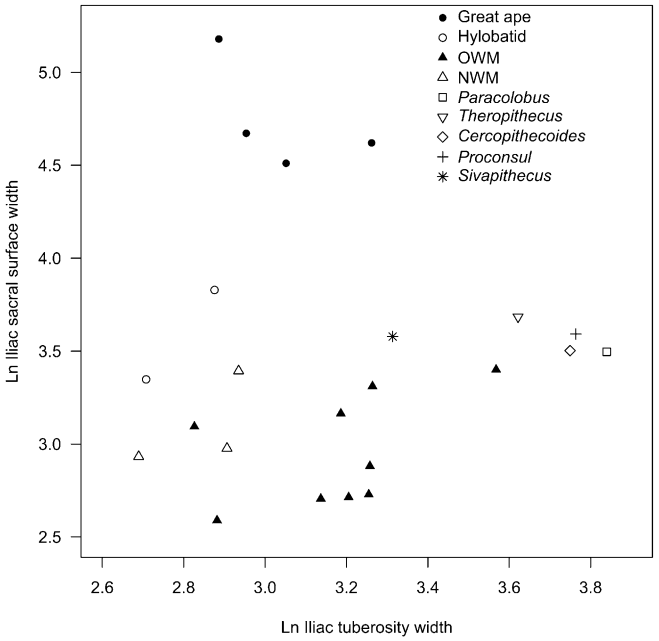

Fig. S2. Bivariate plot of ln iliac sacral surface width (ISW) on ln iliac tuberosity width (ITW). *Cebus* is excluded from this analysis owing to missing data. *Paracolobus*, *Theropithecus*, *Cercopithecoides*, and *Proconsul* data are from Ward (1).

1. Ward CV (1991) Functional anatomy of the lower back and pelvis of the Miocene hominoid *Proconsul nyanzae* from Mfangano Island, Kenya. PhD thesis (The Johns Hopkins Univ, Baltimore).

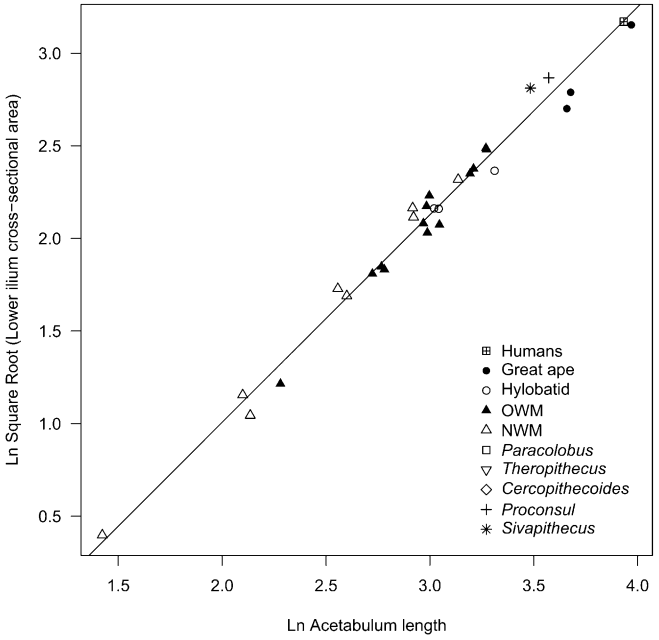

Fig. S3. Reduced major axis fit of ln lower ilium cross-sectional area (LICSA) on ln acetabulum length (AL), $y = 1.12x - 1.24$, $R^2 = 0.98$, $P < 0.0001$ (performed using the smatr package (1) in R (2).

1. Warton DI, Duursma RA, Falster DS, Taskinen S (2012) smatr 3 – an R package for estimation and inference about allometric lines. *Methods Ecol Evol* 3(2):257–259.
2. R Core Team (2013) R: A language and environment for statistical computing. (R Foundation for Statistical Computing, Vienna). Available at www.R-project.org/.

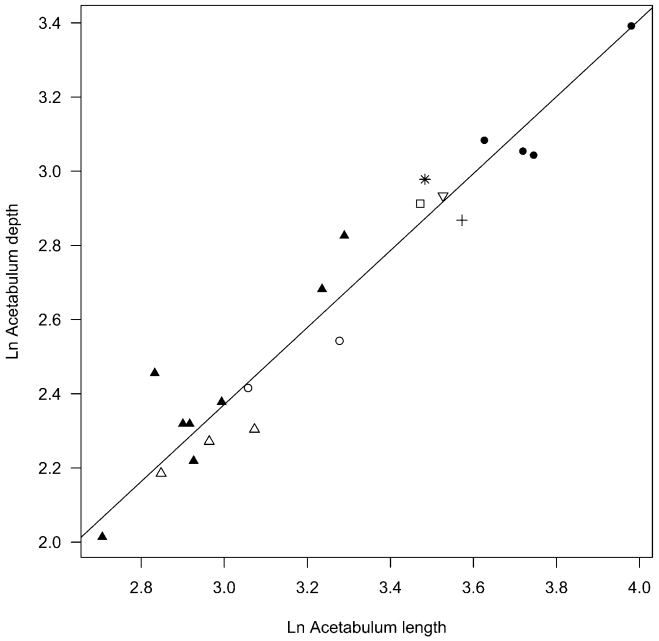

Fig. S4. Reduced major axis fit of ln acetabulum depth (AD) on ln acetabulum length (AL), $y = 1.04x - 0.74$, $R^2 = 0.93$, $P < 0.0001$ [performed using the smatr package (1) in R (2)]. Legend as in Fig. S2.

1. Warton DI, Duursma RA, Falster DS, Taskinen S (2012) smatr 3 – an R package for estimation and inference about allometric lines. *Methods Ecol Evol* 3(2):257–259.
2. R Core Team (2013) R: A language and environment for statistical computing. (R Foundation for Statistical Computing, Vienna). Available at www.R-project.org/.

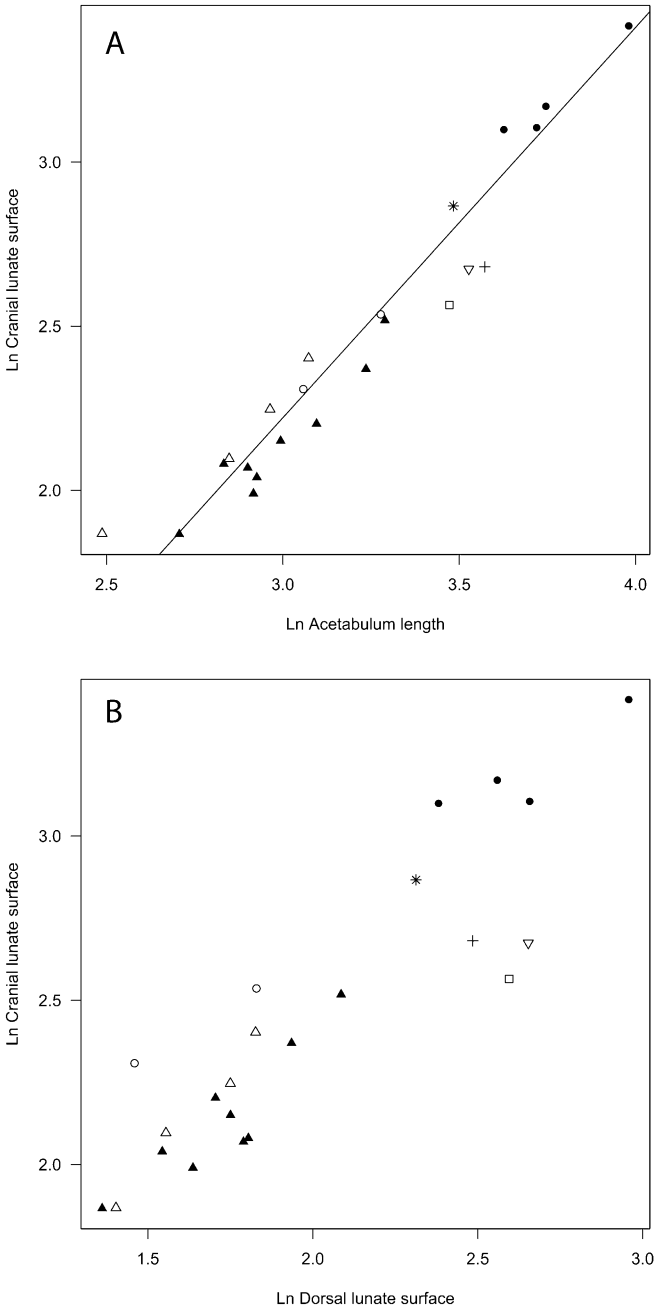

Fig. S5. (*A*) Reduced major axis fit of ln cranial lunate surface width (CLS) on ln acetabulum length (AL), $y = 1.19x - 1.35$, $R^2 = 0.95$, $P < 0.0001$ [performed using the smatr package (1) in R (2)]. (*B*) Ln cranial lunate surface width (CLS) on ln dorsal lunate surface width (DLS) without a regression line. Legend as in Fig. S2.

1. Warton DI, Duursma RA, Falster DS, Taskinen S (2012) smatr 3 – an R package for estimation and inference about allometric lines. *Methods Ecol Evol* 3(2):257–259.
2. R Core Team (2013) R: A language and environment for statistical computing. (R Foundation for Statistical Computing, Vienna). Available at www.R-project.org/.

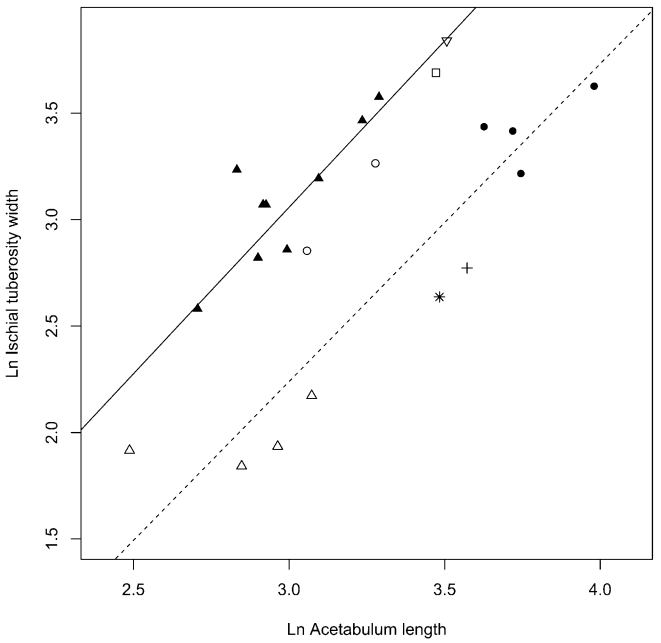

Fig. S6. Bivariate plot of ln ischial tuberosity width (XHTW) on ln acetabulum length (AL). Reduced major axis fits through primates with callosities (solid line, cercopithecoids and hylobatids) and without callosities (dashed line, hominoids and atelids). Callosities: $y = 1.56x - 1.63$, $R^2 = 0.58$, $P = 0.006$; absence of callosities: $y = 1.49x - 2.24$, $R^2 = 0.91$, $P = 0.0002$ [performed using the smatr package (1) in R (2)]. Legend as in Fig. S2.

1. Warton DI, Duursma RA, Falster DS, Taskinen S (2012) smatr 3 – an R package for estimation and inference about allometric lines. *Methods Ecol Evol* 3(2):257–259.
2. R Core Team (2013) R: A language and environment for statistical computing. (R Foundation for Statistical Computing, Vienna). Available at www.R-project.org/.

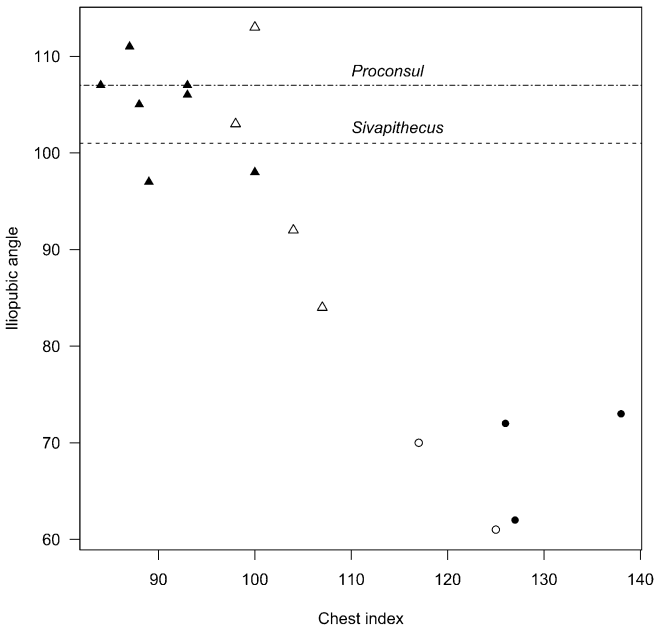

Fig. S7. Bivariate plot of iliopubic angle on chest index [defined as the ratio of the transverse to sagittal dimensions measured at the level of the sternal end of the fourth rib, following Schultz (1)]. Lines denote iliopubic angle values for *Proconsul* and *Sivapithecus*. Legend as in Fig. S2.

1. Schultz A (1956) *Primatologia*, eds Hofer H, Schultz AH, Starck D (Karger, Basel), pp 887–964.

Table S1. Distance matrix of dataset 1 with variables included in Fig. 2

Genus and species	*Alouatta* spp.	*Ateles* spp.	*L. lagotricha*	*E.patas*	*L. albigena*	*M. fascicularis*	*N. larvatus*	*P. cynocephalus*	*P. cristata*	*P. rubicunda*	*P. badius*	*H. lar*	*S. syndactylus*	*P. paniscus*	*P. troglodytes*	*G. gorilla*	*P. pygmaeus*	*P. chemeroni*	*T.oswaldi*	*P. nyanzae*	*S. indicus*
Alouatta spp.	—																				
Ateles spp.	0.31	—																			
Lagothrix lagotricha	0.25	0.46	—																		
Erythrocebus patas	1.26	1.26	1.14	—																	
Lophocebus albigena	1.00	1.11	0.83	0.63	—																
Macaca fascicularis	0.97	0.99	0.88	0.52	0.47	—															
Nasalis larvatus	1.15	1.15	1.08	0.94	0.89	1.01	—														
Papio cynocephalus	1.40	1.33	1.33	0.69	1.01	0.95	0.58	—													
Presbytis cristata	1.02	0.99	0.97	0.83	0.79	0.79	0.38	0.61	—												
Presbytis rubicunda	1.24	1.29	1.12	0.66	0.71	0.87	0.48	0.57	0.58	—											
Procolobus badius	1.90	1.75	1.87	1.05	1.52	1.28	1.32	0.85	1.21	1.32	—										
Hylobates lar	0.71	0.65	0.87	1.45	1.26	1.18	1.06	1.32	0.99	1.35	1.80	—									
Symphalangus syndactylus	1.28	1.10	1.43	1.80	1.83	1.69	1.29	1.43	1.28	1.64	1.80	0.81	—								
Pan paniscus	1.79	1.53	1.91	2.06	2.21	1.99	1.75	1.71	1.62	2.04	1.73	1.48	1.03	—							
Pan troglodytes	2.04	1.77	2.18	2.38	2.54	2.30	2.10	2.05	1.96	2.39	2.02	1.72	1.20	0.41	—						
Gorilla gorilla	3.01	2.76	3.12	3.24	3.47	3.25	2.92	2.85	2.83	3.19	2.75	2.76	2.13	1.35	1.14	—					
Pongo pygmaeus	1.82	1.56	1.93	2.16	2.33	2.12	1.86	1.83	1.75	2.11	1.93	1.59	1.08	0.42	0.48	1.24	—				
Paracolobus chemeroni	1.38	1.33	1.27	0.69	0.91	0.94	0.68	0.54	0.74	0.64	1.00	1.42	1.62	1.95	2.27	3.09	2.06	—			
Theropithecus oswaldi	2.32	2.15	2.30	1.58	2.06	1.87	1.69	1.26	1.66	1.72	0.80	2.18	2.02	1.71	1.96	2.47	1.85	1.43	—		
Proconsul nyanzae	0.96	1.03	0.83	0.99	0.94	1.09	0.91	1.08	0.93	0.82	1.66	1.29	1.62	1.92	2.25	3.02	1.93	1.06	1.94	—	
Sivapithecus indicus	0.55	0.65	0.47	1.06	0.78	0.86	0.98	1.23	0.84	1.03	1.71	0.92	1.48	1.79	2.11	3.02	1.86	1.21	2.10	0.69	—

Table S2. Principal components analysis centroid scores

Genus and species	PC 1	PC 2	PC 3	PC 4	PC 5	PC 6	PC 7	PC 8	PC 9	PC 10	PC 11	PC 12	PC 13	PC 14	PC 15	PC 16
Alouatta spp.	−0.587	−0.739	0.133	−0.218	−0.069	−0.061	−0.061	0.032	0.044	−0.006	−0.001	0.014	−0.016	−0.044	−0.011	−0.014
Ateles spp.	−0.337	−0.628	0.224	−0.188	−0.103	−0.064	−0.110	−0.033	0.028	−0.014	−0.032	0.006	−0.002	0.008	0.005	−0.008
Lagothrix lagotricha	−0.737	−0.625	0.092	−0.340	−0.078	−0.043	−0.099	0.003	−0.039	0.004	0.008	0.034	−0.008	−0.004	−0.008	−0.001
Erythrocebus patas	−0.946	0.446	0.253	−0.188	−0.120	−0.125	0.081	0.049	0.021	0.021	0.123	−0.022	0.023	0.019	−0.015	0.012
Lophocebus albigena	−1.194	−0.007	0.143	−0.170	0.140	0.003	−0.001	−0.019	−0.116	−0.005	0.050	0.008	0.008	0.012	0.006	0.009
Macaca fascicularis	−0.931	0.064	0.463	−0.110	0.049	0.034	0.104	−0.012	0.008	0.033	−0.003	−0.032	0.021	0.022	0.002	−0.003
Nasalis larvatus	−0.644	0.165	−0.450	0.113	0.062	0.066	−0.086	−0.019	−0.012	0.025	−0.020	0.011	−0.007	0.005	−0.011	−0.006
Papio cynocephalus	−0.545	0.576	−0.160	0.113	−0.131	−0.019	0.051	0.005	−0.062	−0.002	−0.001	0.033	−0.008	−0.029	−0.027	−0.006
Presbytis cristata	−0.562	0.141	−0.161	−0.001	0.172	0.213	−0.051	−0.010	0.045	−0.004	0.016	−0.004	−0.007	0.007	−0.008	0.005
Presbytis rubicunda	−0.931	0.329	−0.355	−0.129	−0.052	0.019	0.098	−0.021	0.029	−0.006	−0.010	−0.022	−0.005	−0.016	0.029	−0.002
Procolobus badius	−0.261	1.068	0.409	0.181	−0.011	−0.111	−0.124	0.031	0.040	−0.046	0.001	0.003	0.004	0.019	0.007	−0.006
Hylobates lar	−0.289	−0.661	0.009	0.376	0.046	−0.022	0.028	0.077	−0.017	−0.019	−0.021	−0.007	0.017	0.010	0.002	0.011
Symphalangus syndactylus	0.356	−0.438	−0.224	0.464	−0.283	0.077	−0.013	−0.007	0.057	−0.001	0.000	−0.015	0.013	0.031	0.015	0.002
Pan paniscus	1.002	−0.027	0.073	0.070	0.169	−0.034	0.032	0.014	−0.064	−0.003	−0.020	0.037	0.014	−0.022	0.018	−0.014
Pan troglodytes	1.321	−0.146	0.188	0.139	0.056	−0.046	0.022	−0.031	0.017	0.036	0.031	−0.034	−0.032	−0.022	−0.003	0.018
Gorilla gorilla	2.246	0.224	−0.182	−0.220	−0.018	0.094	−0.052	0.033	0.008	−0.020	0.021	−0.003	0.007	0.015	−0.002	0.001
Pongo pygmaeus	1.101	−0.140	−0.051	−0.161	−0.066	−0.097	0.126	−0.069	−0.006	0.009	−0.031	0.009	0.005	0.005	−0.008	−0.006
Paracolobus chemeroni	−0.780	0.516	−0.115	0.041	−0.152	−0.150	−0.327	−0.204	−0.021	0.015	0.036	−0.040	−0.057	0.050	−0.014	0.038
Theropithecus oswaldi	0.195	1.371	0.103	0.058	0.056	−0.523	−0.040	−0.024	0.035	0.114	−0.021	0.035	−0.059	0.024	−0.037	0.098
Proconsul nyanzae	−0.698	−0.090	−0.322	−0.569	−0.069	−0.296	−0.071	0.266	−0.080	−0.108	0.042	−0.092	−0.060	0.045	0.041	0.009
Sivapithecus indicus	−0.666	−0.424	0.031	−0.357	0.253	−0.181	−0.066	0.141	−0.019	−0.071	0.087	0.107	0.037	−0.007	0.006	0.051

Table S3. Reduced major axis residuals for each logged measure regressed on ln acetabular length (AL)

LICSA		AD		CLS		XHTW (callosities absent)		XHTW (callosities present)	
Pongo pygmaeus	−0.17*	*Procolobus badius*	0.26*	*Cebus apella*	0.26*	*Cebus apella*	0.44*	*Procolobus badius*	0.44*
Sivapithecus indicus	0.14*	*Papio cynocephalus*	0.16*	*Proconsul nyanzae*	−0.22*	*Pan paniscus*	0.26*	*Hylobates lar*	−0.29*
Alouatta caraya	0.13*	*Ateles* spp.	−0.14*	*Pan paniscus*	0.13*	*Lagothrix lagotricha*	−0.25*	*Symphalangus syndactylus*	−0.23*
Saimiri spp.	−0.11*	*Symphalangus syndactylus*	−0.12*	*Presbytis cristata*	−0.13*	*Ateles* spp.	−0.18	*Lophocebus albigena*	−0.19
Symphalangus syndactylus	−0.11*	*Sivapithecus indicus*	0.11*	*Colobus guereza*	−0.13*	*Alouatta* spp.	−0.17	*Presbytis cristata*	0.14
Miopithecus talapoin	−0.11*	*Pongo pygmaeus*	−0.10	*Nasalis larvatus*	−0.13*	*Pongo pygmaeus*	−0.14	*Presbytis rubicunda*	0.13
Macaca nemestrina	0.11*	*Proconsul nyanzae*	−0.10	*Ateles* spp.	0.09	*Pan troglodytes*	0.10	*Erythrocebus patas*	−0.08
Colobus guereza	−0.11*	*Presbytis rubicunda*	−0.08	*Presbytis rubicunda*	−0.09	*Gorilla gorilla*	−0.08	*Papio cynocephalus*	0.07
Pan troglodytes	−0.10	*Nasalis larvatus*	0.07	*Sivapithecus indicus*	0.07			*Nasalis larvatus*	0.04
Proconsul nyanzae	0.10	*Pan troglodytes*	−0.06	*Lagothrix lagotricha*	0.07			*Macaca fascicularis*	−0.02
Cebus albifrons	0.10	*Pan paniscus*	0.06	*Lophocebus albigena*	−0.06			*Colobus guereza*	−0.01
Erythrocebus patas	−0.08	*Lagothrix lagotricha*	−0.06	*Pongo pygmaeus*	0.06				
Lagothrix lagotricha	0.07	*Macaca fascicularis*	−0.05	*Procolobus badius*	0.06				
Procolobus badius	0.06	*Erythrocebus patas*	0.05	*Alouatta* spp.	0.06				
Gorilla gorilla	−0.06	*Presbytis cristata*	0.03	*Papio cynocephalus*	−0.05				
Mandrillus sphinx	0.06	*Alouatta* spp.	−0.03	*Erythrocebus patas*	−0.03				
Cercopithecus mitis	−0.05	*Hylobates lar*	−0.01	*Pan troglodytes*	0.03				
Papio spp.	0.05	*Lophocebus albigena*	0.01	*Gorilla gorilla*	0.03				
Cebuella pygmaea	0.04	*Gorilla gorilla*	0.00	*Hylobates lar*	0.02				
Ateles spp.	0.04			*Symphalangus syndactylus*	−0.02				
Leontopithecus spp.	0.04			*Macaca fascicularis*	−0.01				
Macaca fascicularis	−0.02								
Hylobates hoolock	−0.02								
Nasalis larvatus	0.01								
Cercocebus torquatus	−0.01								
Hylobates lar	0.01								
Cebus apella	0.01								
Chlorocebus aethiops	−0.01								
Theropithecus gelada	0.00								
Homo sapiens	0.00								

*Residual values that fall outside the expected range of one SE based on RMSE (1).

1. Freedman D, Pisani R, Purves R (2007) *Statistics* (Norton, New York), 4th Ed.

Other Supporting Information Files

Dataset S1 (XLSX)